Early Jurassic paleoclimate in Southwest China and its implications for dinosaur fossil distribution

Huan Shen, Laiming Zhang, Chengshan Wang, Romain Amiot, Xu Wang, Linlin Cui, Peng Song

Geological Journal

Early Jurassic paleoclimate in Southwest China and its implications for dinosaur fossil distribution

Journal:	*Geological Journal*
Manuscript ID	GJ-20-0472
Wiley - Manuscript type:	Research Article
Date Submitted by the Author:	28-Nov-2020
Complete List of Authors:	Shen, Huan; China University of Geosciences Beijing, School of Earth Science and Resources Zhang, Laiming; China University of Geosciences Beijing, Wang, Chengshan; China University of Geosciences Beijing, School of the Earth Science and Resources Amiot, Romain ; Université Claude Bernard Lyon 1, Planètes et Environnement Wang, Xu; Chinese Academy of Sciences, Institute of Geology and Geophysics Cui, Lin; Chinese Academy of Sciences, Institute of Geology and Geophysics Song, Peng; National Institute of Natural Hazards
Keywords:	Early Jurassic, dinosaur fossils, Lufeng, stable isotope geochemistry, apatite

Early Jurassic paleoclimate in Southwest China and its implications for dinosaur fossil distribution

Huan Shen [1], Laiming Zhang [1]*, Chengshan Wang [1]*, Romain Amiot [2], Xu Wang [3], Linlin Cui [3], Peng Song [4]

[1] State Key Laboratory of Biogeology and Environmental Geology, China University of Geosciences, Beijing 100083, China, and School of the Earth Science and Resources, China University of Geosciences, Beijing 100083, China

[2] Univ Lyon, Univ Lyon 1, ENSL, CNRS, LGL-TPE, F-69622 Villeurbanne, France

[3] Key Laboratory of Cenozoic Geology and Environment, Institute of Geology and Geophysics, Chinese Academy of Sciences, Beijing 100029, China

[4] National Institute of Natural Hazards, MEMC, Beijing 100085, China

Corresponding author: lzhang@cugb.edu.cn and chshwang@cugb.edu.cn

Abstract

Lufeng County in Southwest China is one of the most famous lagerstätten in which Early Jurassic dinosaurs can be found. The reason of burial for large body size dinosaur fossils at this site is still an enigma, although it could be attributed to either suitable habitats or good preservation conditions. Both of these factors are indirectly regulated by climatic conditions. Therefore, a quantitative reconstruction of the terrestrial paleoclimate of the Lufeng area during the Early Jurassic could help shed new light on this issue. In this study, we analysed the stable isotope compositions of oxygen and carbon ($\delta^{13}C$ and $\delta^{18}O$) in apatite phosphate and carbonate from the tooth

enamel and compact bones of basal sauropodiform and *Sinosaurus* fossils. The oxygen isotopes provided a mean air temperature (MAT) of ≥21 ± 3°C, and the carbon isotopes allowed us to estimate a mean annual precipitation (MAP) of 965 ± 460 mm/yr during the Early Jurassic in Lufeng County. These conditions correspond to a relatively arid tropical savanna climate hospitable to vertebrates life. We also compared the spatial relationship between the global distribution of dinosaur fossils and climatically sensitive deposits during the Jurassic. The dinosaur fossil distribution reveals a strong preference for arid regions. We therefore suggest that "savanna-like" tropical conditions helped accommodate a large number of dinosaurs and preserve their carcasses in the Lufeng area during the Early Jurassic.

Keywords*:* Early Jurassic; dinosaur fossils; Lufeng; stable isotope geochemistry; apatite

1 Introduction

Lufeng County, Yunnan Province, located in southwestern China, holds the main sites of Early Jurassic vertebrate fossils (Fang et al., 2000; Galton & Upchurch, 2004). In this region, several localities have yielded a rich and diverse dinosaur fauna, including non-sauropodan basal sauropodomorphs (Sun & Cui, 1986; Wang, You & Wang, 2017). At least 200 basal sauropodomorph dinosaur individuals belonging to five genera have been excavated, which makes Lufeng County one of the most famous lagerstätten containing Early Jurassic dinosaur fossils in the world (Barrett, Upchurch, & Wang, 2005, 2007a; Langer, Bittencourt, & Schultz, 2010; Wang et al.,

2017; Young, 1941a, 1941b, 1942, 1947, 1951 ; Zhang & Yang, 1995). In addition, other vertebrate fossils such as turtles, lizards, crocodylomorphs, therapsids and mammals, have also been found, indicating the high biodiversity and environmental suitability in this region during the Early Jurassic (Chow & Hou, 1959; Chow, 1962; Crompton & Sun, 1985; Dong, 1990; Hopson, 1964; Patterson & Olson, 1961; Rigney, 1963; Simmons, 1965; Sun & Cui, 1986; Wu, 1991; Wu & Chatterjee, 1993; Zhang & Cui, 1983). The fossils in Lufeng County are also famous for their completeness and exceptional preservation conditions (Luo & Wu, 1994; Young, 1941a). The reason for this large-scale burial of well-preserved dinosaur fossils is of great interest; however, few studies on the subject have been conducted to address this issue. Both the living and burial environments for these vertebrates would be highly regulated or affected by the local paleoclimate. By using an ecological structure analysis, previous studies have claimed that more arid environments tend to favour the preservation of a greater proportion of large-bodied taxa and tend to lack taxa weighing less than 10 kg during the Late Jurassic (Noto & Grossman, 2010). Therefore, it is essential to reconstruct the paleoclimate in Lufeng County during the Early Jurassic to assess this possible taphonomic bias.

The stable oxygen and carbon isotope compositions of mineralized remains of vertebrates (i.e., teeth and bones) can be used to infer their ecological and living environmental conditions (Amiot et al., 2015, 2017; Cullen et al., 2020). The oxygen isotope composition of apatite phosphate ($\delta^{18}O_p$) from terrestrial vertebrate bones and teeth is a function of the oxygen isotope composition of the animal's body water

($\delta^{18}O_{bw}$) as well as that of its body temperature (Amiot et al., 2006; Fricke & Rogers, 2000; Kolodny, Luz, & Navon, 1983; Longinelli, 1984; Luz, Kolodny, & Horowitz, 1984). For most vertebrates, the $\delta^{18}O_{bw}$ value is related to the $\delta^{18}O$ value of ingested water, mainly from plants and drinking water, which is ultimately derived from meteoric water and modified by the animals' physiology and ecology (Kohn, Schoeninger, & Valley, 1996; Straight, Barrick, & Eberth, 2004). The $\delta^{18}O$ value of meteoric water is influenced by temperature, humidity, and the amount of precipitation (Dansgaard, 1964; Fricke & O'Neil, 1999; Grafenstein, Erlenkeuser, Mueller, Trimborn, & Alefs, 1996). Therefore, the climate conditions under which the dinosaurs lived could be recorded in the stable oxygen isotope composition of the apatite phosphate in their skeletal records.

The carbon isotope composition of apatite carbonate ($\delta^{13}C_c$) from terrestrial vertebrate teeth or bones is related to the carbon isotope composition of ingested food, with heavy isotope enrichment that varies depending on the digestive physiology of the animal (Passey et al., 2005). For plant-eating vertebrates, the $\delta^{13}C$ value of the apatite carbonate in their teeth and bones reflects that of their plant diet ($\delta^{13}C_{leaf}$). It is thus possible to estimate the $\delta^{13}C_{leaf}$ value from the $\delta^{13}C_c$ values of plant-eating vertebrate teeth or bones. Combined with the established relationship between the $\delta^{13}C_{leaf}$ value of extant C_3 plants and mean annual precipitation (MAP), MAP values can be inferred from the apatite carbonate $\delta^{13}C_c$ values of vertebrates (Amiot et al., 2015). In this study, we apply these oxygen and carbon isotope proxies to dinosaur teeth and bones from Lufeng County to reconstruct the Early Jurassic paleoclimatic

conditions in terms of mean air temperature and mean amount of precipitation.

In this study, we also examine the spatial relationships between the global distribution of dinosaur fossils and climatically sensitive deposits to explore the climatic (arid and humid) preference of Jurassic dinosaurs. Proxies based on climatically sensitive deposits have been widely applied to estimate arid and humid regimes (Boucot, Xu, & Scotese, 2013; Porada et al., 2016; Torsvik & Cocks, 2016; William & Sascha, 2012; Zhang et al., 2016). For example, the formation of coal needs abundant rainfall and usually develops under specific climatic conditions, such as in tropical rainforests or temperate forests (Craggs, Valdes, & Widdowson, 2012; Izart et al., 2012; Utescher, Ashraf, Kern, & Mosbrugger, 2020). We believe that the combination of a local quantitative terrestrial paleoclimate reconstruction and the analysis of the global qualitative spatial contrast between the global distribution of dinosaur fossils and climatically sensitive deposits using ArcGIS software during the Jurassic could help to shed new light on the enigma of the burial of large quantity of dinosaur fossils.

2 Geological setting

Lufeng Basin, Yunnan Province, Southwest China (25.15 °N, 102.08 °E) was located between 30° N and 40° N during the Early Jurassic (Huang, 2005) (Figure 1). It is a back-arc basin caused by the subduction-collision of the Yangtze Block during the Late Triassic-Jurassic (Chen, Hu, Qu, & Wu, 2011). The sedimentary sequence preserved in the Lufeng Basin comprises the Lower Jurassic Lufeng Formation (the

Shawan and Zhangjia'ao members), the Middle Jurassic Chuanjie and Laoluocun members, and the Upper Jurassic Madishan and Anning members, from bottom to top (Fang et al. 2000; Huang, 2005; Figure 2). The fine-grained sediments of the Lufeng Formation contain a large number of Early Jurassic dinosaur fossils. It is characterized by red and purple-red fine-grained sediments with small amounts of interlayer limestone (Figure 2), which represents a shallow lacustrine environment. The widespread paleosol carbonate nodules suggest an arid or semiarid climate during the deposition of the Lufeng Formation. Starting at the beginning of the 1940s, numerous dinosaur fossils, as well as footprints, have been collected in Lufeng Basin. These dinosaur fossils are relatively well preserved and densely distributed, and the Lufeng Formation includes for the sauropodomorphs *Lufengosaurus* (Barrett et al., 2005; Young 1941a, 1951), *Yunnanosaurus* (Barrett et al. 2007b; Young 1942), *Jingshanosaurus* (Zhang & Yang, 1995), and *Xixiposaurus* (Sekiya, 2010), an unnamed basal sauropod (= "Yizhousaurus"; Chatterjee et al., 2010), and some theropods (e.g., Hu, 1993; Wu, Currie, Dong, Pan, & Wang, 2009) and ornithischians (e.g., Irmis & Knoll 2008). .

3 Material and methods

3.1 Material

In this study, two teeth and two bones collected from the Lufeng Formation were analysed[1] (Table 1). The studied samples consist of two bones (LFB01 and LFB02)

[1] The fossils were donated by the Lufeng Dinosaurian Museum.

and one tooth (LFT06) of a basal sauropodiform and one tooth (ZGT09) of the theropod *Sinosaurus triassicus*. The tooth of the herbivorous basal sauropodiform shows a typical "flat and blunt leaves" shape since its primary function was grinding, cutting, or shearing (Galton, 1985; Figure 3). The tooth of the carnivore *Sinosaurus* (Dinosauria: Theropoda) has typical predatory/scavenger characteristics with fine serrations at the edges (Xing et al., 2013).

The well-preserved hard parts of the teeth and compact bones were powdered by using a dental drill. For each bone, powders drilled from different locations were mixed. For each tooth, the powder from the apex and cervix were collected and analysed separately.

3.2 Methods

3.2.1 Measurements of oxygen and carbon isotope compositions of apatite phosphate and carbonate

Apatite powders from dinosaur teeth and bones were treated following the protocol described in Lécuyer (2004). This protocol consists of the isolation of phosphate (PO_4^{3-}) from apatite as silver phosphate (Ag_3PO_4) crystals using acid dissolution and an anion-exchange resin. For each sample, 20-30 mg of enamel powder was dissolved in 2 mL of 2 M HF. The CaF_2 residue was separated by centrifugation and the solution was neutralized by adding 2.2 mL of 2 M KOH. Amberlite™ anion-exchange resin beads were added to the solution to isolate the

PO_4^{3-} ions. After 24 h, the solution was removed, and the resin was rinsed and eluted with 27.5 mL of 0.5 M NH_4NO_3. After 4 h, 0.5 mL of NH_4OH and 15 mL of an ammonia solution of $AgNO_3$ were added, and the solutions were placed in a thermostatic bath at 70°C for 7 h, allowing the precipitation of Ag_3PO_4 crystals. The oxygen isotope compositions of the silver phosphate crystals were measured using a high temperature elemental analyser equipped with "purge and trap" technology interfaced in continuous flow mode to an isotopic ratio mass spectrometer at the Laboratoire de Géologie de Lyon (UMR 5276, Université Claude Bernard Lyon 1). For each sample, 5 aliquots of 300 µg of Ag_3PO_4 were mixed with 300 µg of pure graphite powder loaded in silver foil capsules. Pyrolysis was performed at 1450°C with a glassy carbon reactor using a varioPYROcube™ Elemental Analyser interfaced in continuous flow mode with an Isoprime™ isotopic ratio mass spectrometer. The measurements were calibrated against silver phosphate precipitated from NBS120c (natural Miocene phosphorite from Florida), as well as against NBS127 (barium sulfate precipitated using seawater from Monterey Bay, California, USA). The value of NBS120c was fixed at 21.7‰ (V-SMOW; Vienna Standard Mean Ocean Water) according to Lécuyer, Grandjean, O'Neil, Capetta, and Martineau. (1993), and that of NBS127 set at the value of 9.3‰ V-SMOW (Hut, 1987) for the correction of the instrumental mass fractionation during CO isotopic analysis. The silver phosphate precipitated from the standard NBS120c along with the silver phosphate samples derived from the fossil bioapatites was repeatedly analysed ($\delta^{18}O_p$ = 21.7 ±0.1‰, n = 4) to ensure that no isotopic fractionation occurred during the wet chemistry. Data are

reported as $\delta^{18}O$ values vs. V-SMOW (in ‰ δ units).

Approximately 10 mg of enamel, or bone powder was pre-treated according to the procedure of Koch, Tuross, and Fogel. (1997). To remove organic matter and dibasic carbonates, the powder was cleaned with a 2% NaOCl solution followed by being treated using a 0.1 M acetic acid solution. Each treatment lasted for 24 h. The samples were rinsed five times with distilled water. Afterward, at Laboratory for Environment Isotope Geochemistry, Institute of Geology and Geophysics, Chinese Academy of Sciences, the samples were analysed using a Thermo Finnigan Gasbench II coupled with MAT253 continuous flow isotope ratio mass spectrometer, following a procedure adapted from the methods outlined in Spoetl and Vennemann (2003). Five drops of 100% orthophosphoric acid were added and the samples were allowed to react at 72°C in helium for 1 h. After that, 10 measurements of the isotopic composition of the resulting carbon dioxide. The measured carbon and oxygen isotopic compositions were normalized relative to the NBS-19 calcite standard with the addition of calcite CO_2-carbonate acidic fractionation factors. The reproducibility of the carbon and oxygen isotope compositions of the carbonate apatite was better than ±0.1‰ and ±0.2‰, respectively. The carbon and oxygen isotopic compositions are reported relative to the V-PDB and V-SMOW, respectively (in ‰ δ units).

3.2.2 Data compilation of dinosaur fossils and climatically sensitive deposits

Using the Paleobiology Database (https://paleobiodb.org/), a dataset of Jurassic dinosaur fossil sites was compiled (Appendix 1). This study focuses on the burial

environments of fossil bones, excluding dinosaur eggs and tracks in this data compilation. These fossil sites are classified into two groups according to their stratigraphic age (i.e., Lower-Middle Jurassic and Upper Jurassic). The paleolatitude and paleolongitude for each site provided by the database were also used.

Climatically sensitive deposit markers corresponding to two time slices, the Early-Middle Jurassic and the Late Jurassic were compiled from the Lithologic Atlas according to Boucot et al. (2013). In our compilation, evaporites, gypsums, and calcretes were regarded as arid indicators, while coals seam were regarded as humid indicators. The paleolatitude and paleolongitude during the Early-Middle Jurassic (180 Ma) and Late Jurassic (150 Ma) for each deposit are calculated by using PointTracker software.

Each locality was plotted on a paleogeographic map (180 and 150 Ma reconstructions) using PALEOMAP PaleoAtlas raster mapping in ArcGIS software.

4 Results

4.1 Oxygen and carbon isotope compositions of apatite phosphate and carbonate

For the basal sauropodiforms, the $\delta^{18}O_p$ values ranged from 15.9‰ to 20.5‰ with an average value of 17.6±0.2‰, and the $\delta^{13}C_c$ values ranged from -10.6‰ to -8.7‰, with an average value of -9.5±0.1‰. For the *Sinosaurus* specimens, the $\delta^{18}O_p$ values ranged from 17.0‰ to 20.4‰, with an average value of 18.7±0.2‰, and the $\delta^{13}C_c$ values ranged from -7.8‰ to -7.1‰, with an average value of -7.4±0.1‰ (Table 1).

4.2 The distribution of dinosaur fossils and climatically sensitive deposits

In our database, 594 fossil sites and 829 climatically sensitive deposit markers were compiled (Appendix 1; Figure 4).

For the Early-Middle Jurassic, 408 dinosaur fossil sites and 591 climatically sensitive deposit markers were compiled. The arid zones occurred in southern North America, most of South America, and the majority of Africa and the Persian Gulf region. There were also scattered arid areas in South Asia. Humid belts are prominent at higher latitudes of the Northern Hemisphere and in Australia in the Southern Hemisphere. The dinosaur fossils are mostly distributed at middle and low latitudes, including in southern North America and in the shallow continental shelves of South America and Africa, with scattered fossil sites in central Asia. However, at mid- and high latitudes, dinosaur fossils are scarce. We noticed that the majority of dinosaur fossil sites were associated with arid climatic markers, especially in southern North America and northern South America.

For the Late Jurassic, 186 dinosaur fossil sites and 238 climatically sensitive deposit sites were collected. A Northern Hemisphere arid belt that extends from eastern North America through southern Russia, Central Asia, and parts of southwestern and northern China to southern England can be observed. This arid belt is also a major zone for dinosaur fossil occurrences. The humid zone is mainly located in South America, Australia, the Indian Peninsula, and southern South America, in a state of dissimilarity with most dinosaur fossil sites. The dinosaur fossils are mainly

distributed in middle and lower latitudes, especially at the regions near the equator (Figure 4).

5 Discussion

5.1 Preservation of dinosaur teeth and bone stable isotope compositions

The stable oxygen and carbon isotope compositions of vertebrate remains can be altered by the diagenetic conditions (e.g., fracturing, fluid circulation, and metamorphism) and chemical properties (e.g., temperature, pH, and Eh) of the burial environment. Diagenetic alteration mainly occurs through the dissolution-reprecipitation mechanism, which can be either microbially mediated or induced by mineral-fluid interactions (Lécuyer, Grandjean, & Sheppard, 1999; Zazzo, Lécuyer, & Mariotti, 2004a). Compared to other vertebrate remains, enamel is more reliable and prone to resisting diagenetic alteration as a result of its larger and more densely packed apatite crystals, lower organic matter content, and lower porosity (Fricke & Pearson, 2008; Stanton-Thomas & Carlson, 2004). In addition, it has been shown that compact bone can also be a reliable material used to archive original isotopic compositions (Kohn & Cerling, 2002; Longinelli, 1984; Luz et al., 1984; Tütken, Pfretzschner, Vennemann, Sun, & Wang, 2004).

In the case of equilibration with diagenetic fluids, it would be expected that the isotopic compositions of different taxa would tend to homogenize towards the value of the diagenetic source. Lécuyer et al. (2003) suggested that the original information could be altered if the difference between the isotopic values of different taxa is less

than 1‰. In this study, the difference between isotopic values of the basal sauropodiform and *Sinosaurus* is larger than 1‰, which suggests that our samples were not homogenized during burial.

Based on a summary of the isotopic values of the teeth and bones of modern vertebrates, Rey, Amiot, and Fourel (2017) proposed a method to distinguish vertebrate remains that have preserved their stable oxygen isotope composition of apatite. First, inorganic carbonate precipitated from diagenetic fluids would lead to a carbonate content in apatite higher than 13.4%, as the naturally occurring apatite-bound carbonate content of extant vertebrates does not exceed this value (Rey et al., 2017). Second, microbially-mediated diagenetic alteration of apatite phosphate leads to a difference between $\delta^{18}O_p$ and $\delta^{18}O_c$ exceeding 14.7‰ (Vennemann, Hegner, Cliff, & Benz, 2001; Zazzo, Lécuyer, Sheppard, Grandjean, & Mariotti, 2004b; Figure 5). In this study, all the $\delta^{18}O_p$ - $\delta^{18}O_c$ values were lower than 14.7‰ and the carbonate contents of our samples were less than 13.4% (Figure 3). Therefore, we suggest that our samples have at least partially maintained their original oxygen and carbon isotope compositions and could be interpreted in terms of the paleoecology and living environment of the Early Jurassic dinosaurs in Lufeng County.

5.2 Early Jurassic terrestrial paleoclimate in Lufeng County

5.2.1 Temperature and precipitation

The $\delta^{18}O$ value of meteoric water ($\delta^{18}O_w$), which constitutes a major source of drinking water for terrestrial vertebrates can be used to calculate the mean air

temperature using a modern relationship relating the mean $\delta^{18}O_w$ value of precipitation to the mean annual air temperature (MAAT), such as the relationship proposed in Amiot et al. (2004):

$$\delta^{18}O_w = 0.49(\pm0.03) \times T - 14.18(\pm0.52) \quad (1)$$

with T being the MAAT value in °C. Using the phosphate-water oxygen isotope fractionation equation established for extant vertebrates, it is possible to estimate the $\delta^{18}O_w$ value of meteoric water from the $\delta^{18}O_p$ value of apatite phosphate. For dinosaurs, the $\delta^{18}O$ value of meteoric water ($\delta^{18}O_w$) could be estimated using the present-day relationships established between birds, the closest living relatives to dinosaurs, and meteoric water (equation 2; Amiot et al., 2017); this estimation has been recently tested on Cretaceous dinosaurs (Amiot et al., 2020).

$$\delta^{18}O_w = 1.119(\pm0.04) \times \delta^{18}O_p - 24.222(\pm0.644)\ R^2=0.98 \quad (2)$$

In this study, the average $\delta^{18}O_p$ value is 18.2±0.1‰. Using equation 1, the average $\delta^{18}O_w$ value is -3.9±0.94‰. Assuming that the meteoric water cycle of the Early Jurassic did not differ drastically compared with the modern cycle, the modern relationship between the mean annual air temperature (MAAT) and $\delta^{18}O_w$ value (equation 2) can be applied to provide a temperature value for the Early Jurassic in Lufeng County of 21±3°C (Table 2).

According to Diefendorf, Mueller, Wing, Koch, and Freeman. (2010), a significant relationship exists between the average $\delta^{13}C$ values of C_3 plants and the local mean annual precipitation (equation 3):

$$log_{10}(MAP) = 0.0802(\pm0.0102) \times \Delta^{13}C_{leaf} + 1.3726(\pm0.1875);\ R^2=0.44 \quad (3)$$

with $\Delta^{13}C_{leaf} = (\delta^{13}C_{atm} - \delta^{13}C_{leaf})/(1+\delta^{13}C_{leaf}/10^3)$. To estimate an average $\delta^{13}C$ value for local plants, the $\delta^{13}C_c$ value of apatite carbonate from the teeth and bones of herbivorous dinosaurs can be used by applying the carbonate-diet ^{13}C enrichment established for plant-eating animals. Using the carbon isotope compositions of the plant-derived organic matter of the sediment bearing dinosaur teeth, Tütken (2011) estimated an apatite-diet ^{13}C-enrichment close to 16‰ for sauropods. Although their phylogenetic position is still debated, basal sauropodiforms are believed to be the ancestors of sauropods (Barrett et al., 2005). Therefore, we assume in this study that the carbon isotope fractionation between local plants and basal sauropodiform apatite is 16‰. In this way, the inferred $\delta^{13}C$ values of the diet (plants) of basal sauropodiform range from -28.8‰ to -23.8‰, which is consistent with the $\delta^{13}C$ values of modern C_3 plants (-20‰ to -35‰). The carbon isotope composition of atmospheric CO_2 ($\delta^{13}C_{atm}$) can also be estimated using the relationship established between the $\delta^{13}C$ value of oceanic carbonates and that of atmospheric CO_2 (Passey et al., 2002):

$$\delta^{13}C_{atm} = \delta^{13}C_{oceanic\ carbonates} - 7.9‰$$

Because the $\delta^{13}C_{oceanic\ carbonate}$ value was approximately 2 ‰ during this time period (Morettini et al., 2002), the estimated $\delta^{13}C_{atm}$ value was approximately -5.9‰ during the Early Jurassic. Using equation 3, the calculated Early Jurassic MAP in Lufeng County was 965 ± 460 mm.

It is worth noting that the difference in oxygen isotopes between the apex and the cervix of the *Sinosaurus* tooth is 3.4‰ (ZGT09-1A and ZGT09-2A; Figure 6). We

assume that this difference may be attributed to seasonal variations in temperature or precipitation. Due to the subtropical paleolatitude of the Lufeng area during the Early Jurassic, such a change may affected by both seasonal changes in the precipitation regime as well as by variations in temperature, as the wet season being characterized by lower water $\delta^{18}O$ values as a result of the elevated amount of precipitation (the so-called amount effect; Amiot et al., 2009; Dansgaard, 1964). However, temperature may overprint this tendency by raising the $\delta^{18}O$ values of meteoric water during the warmest months, leading to either a large seasonal amplitude in $\delta^{18}O$ values if the hot season coincides with the dry season, or a small amplitude if the warm season coincide with the rainy season.

5.2.2 Climatic zone characterzation

According to the paleoclimate classification proposed by Zhang et al. (2016), Lufeng County had a tropical savanna climate during the Early Jurassic Few freshwater bivalves are found in individual areas, characterized by thick-shelled types adapted to warm environments belonging to the *Eolamprotula-Cuneopsis-Psilunio* faunal assemblage. In addition, pollen data *Classopllis* was observed to be of high content, reflecting an arid climate (Deng et al., 2017). Today, this climate dominates many low latitude regions such as parts of the African continent, the northern parts of South America, Australia, and parts of Asia (e.g., India). The average annual rainfall amount in this climate zone is relatively low, varying between 800 and 1,600 mm and decreasing with increasing latitude (Leong, 1995). Based on modern observation, the

climate in tropical savannas shows alternating arid and humid seasons called wet and dry climates due to the influence of trade winds. There is a huge difference in precipitation between summer and winter. In summer, onshore winds bring rain, and in winter, offshore winds keep the savanna arid. In the driest months of winter, the precipitation amount is less than 60 mm (Leong, 1995). The average monthly temperature is >18°C throughout the year, and temperatures are higher during the rainy season. The temperatures are 25-30°C during the rainy season and 20-25°C during the arid season (Leong, 1995).

Under such climate conditions, the natural vegetation in tropical savannas primarily consists of tall grasses and short deciduous trees. These trees shed their leaves during periods of drought to reduce the loss of water by transpiration. They also tend to have wide trunks that can store additional water to help them survive during prolonged drought. Local vertebrate species richness is about almost the same level between tropical savannas and tropical forests (Murphy, Andersen, & Parr, 2016). For terrestrial animals, large size influences their movement in dense forests, therefore the open environment of the savannas is more conducive to large animal species. As a result, the savanna climate accommodates a wide range of animal sizes and high biodiversity (Noto & Grossman, 2010). It can be inferred that the Lufeng area, similarly to the current African savanna, was highly rich in biodiversity. Indeed, in addition to dinosaur fossils, mammals and other vertebrates are abundant (Chow and Hou, 1959; Chow, 1962; Crompton & Sun, 1985; Dong, 1990; Hopson, 1964; Patterson & Olson, 1961; Rigney, 1963; Simmons, 1965; Sun & Cui, 1986; Wu 1991;

Wu & Chatterjee, 1993; Zhang & Cui, 1983). A climatic environment similar to a tropical savanna might account for the high diversity of fossil species in Lufeng. Besides, open environment like savannas are more suited for larger animals. Therefore, the Lufeng County might have a greater proportion of large-bodied taxa like basal sauropodiform and lack anything smaller than 10 kg due to its savanna-like paleoenvironment (Noto & Grossman, 2010).

5.3 Spatial relationships between dinosaur fossils and climatic regimes

Gardner et al. (2016) suggested that warm and humid conditions were beneficial to avian fossil burial after evaluating avian fossils from the Jurassic and Cretaceous. Most of the bodies suffered weathering and then underwent a long period of petrification. Warm and humid temperatures are conducive to the preservation of intact avian fossils, which contradicts the common view that drought is better for fossil preservation. Therefore, it is necessary to test the wet and dry distribution of Jurassic dinosaur fossils.

To evaluate the spatial relationship between dinosaur fossils and climatically sensitive deposits, standard deviational ellipses (SDEs) of the dinosaur fossils, arid indicators, and humid indicators are drawn for each time slice (Figure 7). An SDE is a graphical representation of the standard deviation along the X and Y axes, centred on the average geometric data for all positions. In two-dimensional space, the point distribution has two directions: (1) centralization (centralized trend) and (2) spread (dispersion). The central tendency and dispersion refer to the diffusion of the average

centre bounded by an ellipse (Rahmaniati et al., 2014). The purpose is to provide a summary of the trend and to check whether the dispersion of the data is biased against the distribution points. The rotation and intersection areas, as well as the distance of the ellipse gravity centres between the fossils and humid/arid indicators are obtained, aiming to describe the tendency of fossils distributed among different climate conditions. A smaller rotation, a larger intersection area, and a shorter distance from the centre of gravity represent a stronger correlation, and vice versa.

The following comparisons are based on arid zone vs. dinosaur occurrence and humid zone vs. dinosaur occurrence, and for ease of reading we abbreviate the former as A-D and the latter as H-D. If we represent a difference in value, we use D(A-D) for the difference value between the arid zone and dinosaur occurrence and D(H-D) for the difference value between the humid zone and dinosaur occurrence.

In Figure 8, the SDE rotation angles of D(A-D) and D(H-D) are 9.57 and 4.78 degrees during the Early-Middle Jurassic, respectively, and -8.83 and -7.93 degrees during the Late Jurassic, respectively. This suggests that the distribution of dinosaur fossils is consistent with the climate regimes and does not deviate from the general direction of the climate regimes. During the Early-Middle Jurassic, the distances between the ellipse gravity centres of D(A-D) and D(H-D) are 3.3E+6 and 5.6E+6, respectively. During the Late Jurassic, these distances are 4.5E+5 and 4.6E+6, respectively. During the Jurassic, dinosaur fossils had a closer spatial relationship to the arid regime, which suggests that an arid climate is conducive to the preservation of the dinosaur fossils. The intersection area of the SDE shows that 81% of the arid

regime and 47% of the humid regime contained dinosaur fossils from the Early-Middle Jurassic, while the shares are 85% and 38% for the Late Jurassic. This suggests that sites with arid climates would have a higher possibility of yielding dinosaur fossils.

Overall, the results of the SDEs showed that an arid climate seems to provide better conditions than does a humid climate for fossil preservation on a global scale.

Conclusion

The oxygen and carbon isotope compositions of dinosaur apatites recovered from Southwest China suggested that the MAT was 21± 3°C and the MAP was 965±460 mm during the Early Jurassic. The inferred warm and dry climatic condition corroborates the tropical savannas landscape in the region as revealed by pollen and bivalves data in previous study. The tropical savannas climate indicates that the Lufeng county may develop with a distinct humid and arid season in the Early Jurassic. We also compared the spatial distribution of global dinosaur fossils with that of climatically sensitive deposits during the Jurassic. It showed that the dinosaur fossils had a strong preference for distributing over arid regions. Therefore, we suggest that relatively arid tropical savannas favoured the accommodation of a large number of dinosaurs and the preservation of such a high number of carcasses in the Lufeng area during the Early Jurassic. This study provides for the first time a quantitative climatic condition under which the dinosaurs lived in the Lufeng county.

Acknowledgments

We thank T. Wang from the Lufeng Dinosaurian Museum for supplying the materials. We thank Q. Wang, S. Cao, and J. Tan for their help during the fieldwork. We also want to thank L. Xing for providing helpful suggestions. This study was financially supported by the National Key R&D Plan of China (grant 2018YFE0204204), National Natural Science Foundation of China (grant 41790455), the Chinese "111" project (grant B20011), the China Geological Survey Program (grant DD20190685), and the Fundamental Research Funds for the Central Universities (grant 2652018130).

References

Amiot, R., Angst, D., Legendre, S., Buffetaut, E., Fourel, F., Adolfssen, J., …, Lécuyer, C. (2017). Oxygen isotope fractionation between bird bone phosphate and drinking water. *The Science of Nature, 104*, 47.

Amiot, R., Kusuhashi, N., Saegusa, H., Shibata, M., Ikegami, N., Shimojima, S., ..., Lécuyer, C. (2020). Paleoclimate and ecology of Cretaceous continental ecosystems of Japan inferred from the stable oxygen and carbon isotope compositions of vertebrate bioapatite. Journal of Asian Earth Sciences 104602. https://doi.org/10.1016/j.jseaes.2020.104602

Amiot, R., Lécuyer, C., Buffetaut, E., Fluteau, F., Legendre, S., & Martineau, F. (2004). Latitudinal temperature gradient during the Cretaceous Upper Campanian-Middle Maastrichtian: $\delta^{18}O$ record of continental vertebrates. *Earth Planet. Sci. Lett. 226*, 255–272.

Amiot R, Lécuyer C, Buffetaut E, Escarguel G, Fluteau F, & Martineau F. (2006). Oxygen isotopes from biogenic apatites suggest widespread endothermy in Cretaceous dinosaurs. *Earth Planet Sci Lett., 246*, 41–54.

Amiot, R., Wang, X., Zhou, Z., Wang, X., Lécuyer, C., Buffetaut, E., ..., Xu, X. (2015). Environment and ecology of East Asian dinosaurs during the Early Cretaceous inferred from stable oxygen and carbon isotopes in apatite. *J. Asian Earth Sci., 98*, 358–370.

Amiot, R., Buffetaut, E., Le, C., Fernandez, V., Fourel, O. I. S., Cedex, V., & Cedex, P. (2009). Oxygen isotope composition of continental vertebrate apatites from Mesozoic formations of Thailand. *Geological Society, London, Special Publications, 315*(1), 271-283.

Barrett, P.M., Upchurch, P., & Wang, X.L. (2005). Cranial osteology of Lufengosaurus huenei Young (Dinosauria: Prosauropoda) from the Lower Jurassic of Yunnan, People's Republic of China. *Journal of Vertebrate Paleontology, 25*, 806-822.

Barrett, P. M., Upchurch, P., Zhou, X.D., & Wang, X.L. (2007a). The skull of Yunnanosaurus huangi Young, 1942 (Dinosauria: Prosauropoda) from the Lower Lufeng Formation (Lower Jurassic) of Yunnan, China. *Zoological Journal of the Linnean Society, 150*(2), 319–341.

Barrett, P. M., & Upchurch, P. (2007b). The evolution of feeding mechanisms in early Sauropodomorph dinosaurs. *Palaeontology, Special Papers 77*, 91-112.

Boucot, A.J., Xu, C., & Scotese, C.R. (2013). Phanerozoic paleoclimate: An atlas of lithologic indicators of climate, Phanerozoic Paleoclimate.

Chatterjee, S., Wang, T., Pan, S.G., Dong, Z., Wu, X.C., & Upchurch, P. (2010). A complete skeleton of a basal sauropod dinosaur from the early Jurassic of China and the origin of Sauropoda. *Geological Society of America Abstracts with Programs, 42* (5), 26.

Chen, H., Hu, J. M., Qu, H. J., & Wu, G. L. (2011). Early Mesozoic structural deformation in the Chuandian N-S Tectonic Belt. *China. Sci. China Earth Sci. 54*, 1651–1664.

Chow, M. (1962). A tritylodont specimen from Lufeng, Yunnan. *Vertebrata Palasiatica, 6*, 365-367.

Chow, M., & Hou, C. C. (1959). A new tritylodont from Lufeng, Yunnan. *Vertebrata Palasiatica, 3*, 9-12.

Craggs, H. J., Valdes, P. J. & Widdowson, M. (2012). Climate model predictions for the latest Cretaceous: An evaluation using climatically sensitive sediments as proxy indicators. *Palaeogeography, Palaeoclimatology, Palaeoecology, 315–316*(0), 12-23.

Crompton, A. W., & Sun, A L. (1985). Cranial structure and relationships of the Liassic mammal

Sinoconodon. *Zoological Journal of the Linnean Society, 85*, 99-119.

Cullen, T. M., Longstaffe, F. J., Wortmann, U. G., Huang, L., Fanti, F., Goodwin, M. B., …, Evans, D. C. (2020). Large-Scale Stable Isotope Characterization of a Late Cretaceous Dinosaur-Dominated Ecosystem. *Geology, 48*(6), 546–51.

Dansgaard, W. (1964). Stable isotopes in precipitation. *Tellus, 16*, 436–468.

Deng, S. H., Lu, Y. Z., Zhao, Y., Fan, R., Wang, Y. D., Yang, X. J., …, Sun, B. N. (2017). The Jurassic paleoclimate regionalization and evolution of China. *Earth Science Frontiers, 24*(1), 106–142.

Diefendorf, A. F., Mueller, K. E., Wing, S. L., Koch, P. L., & Freeman, K. H. (2010). Global patterns in leaf ^{13}C discrimination and implications for studies of past and future climate. *Proc. Natl. Acad. Sci., 107*, 5738–5743.

Dong, Z. M. (1990). Stegosaurs of Asia. In: Carpenter K and Currie P J, eds. Dinosaur Systematics. Cambridge University Press, Cambridge. 255-268.

Fang, X., Long, Q., Lu, L., Zhang, Z., Pan, S., Wang, Y., …, Cheng, Z. (2000). Lower, Middle, and Upper Jurassic subdivision in the Lufeng region, Yunnan Province. *In Third National Stratigraphical Congress of China*, 208–214. Geological Publishing House Beijing.

Fricke, H.C., & O'Neil, J.R. (1999). The correlation between $^{18}O/^{16}O$ ratios of meteoric water and surface temperature: its use in investigating terrestrial climate change. *Earth Planet. Sci. Lett., 170*, 181–196.

Fricke, H.C., & Rogers, R. R. (2000). Multiple taxon-multiple locality approach to providing oxygen isotope evidence for warm-blooded theropod dinosaurs. *Geology, 28*, 799–802.

Fricke, H.C., & Pearson, D. A. (2008). Stable isotope evidence for changes in dietary niche partitioning among hadrosaurian and ceratopsian dinosaurs of the Hell Creek Formation, North Dakota. *Paleobiology, 34*, 534–552.

Galton, P. M. (1985). Diet of prosauropod dinosaurs from the late Triassic and early Jurassic. *Lethaia*, 18, 105-123.

Galton, P. M., & Upchurch, P. (2004). In The Dinosauria, Second Edition (eds Weishampel, D. B., Dodson, P. & Osmólska, H.). CA: University of California Press, 232–258.

Hopson, J. A. (1964). The braincase of the advanced mammal- like reptile Bienotherium. *Postilla, 87*,1-30.

Hu, S. J. (1993). A short report on the occurrence of Dilophosaurus from Jinning County, Yunnan Province. *Vertebrata PalAsiatica, 31*: 65–69.

Huang, B. C. (2005). Jurassic magnetic stratigraphy in Lufeng area, central Yunnan. *Chinese geological bulletin, 24*, 322-328. (In Chinese)

Hut, G. (1987). Consultants' group meeting on stable isotope reference samples for geochemical and hydrological investigations. *Journal of Geophysical Research*, 42.

Irmis, R.B. & Knoll, F. (2008). New ornithischian dinosaur material from the Lower Jurassic Lufeng Formation of China. *Neues Jahrbuch für Geologie und Paläontologie, Abhandlungen, 247*, 117–128.

Izart, A., Palhol, F., Gleixner, G., Elie, M., Blaise, T., Suarez-Ruiz, I., ..., Panova, E. A. (2012). Palaeoclimate reconstruction from biomarker geochemistry and stable isotopes of n-alkanes from Carboniferous and Early Permian humic coals and limnic sediments in western and eastern Europe. *Organic geochemistry*,*43*, 125-149.

Koch, P. L., Tuross, N., & Fogel, M. L. (1997). The effects of sample treatment and diagenesis on the isotopic integrity of carbonate in biogenic hydroxylapatite. *Journal of Archaeological Science, 24*, 417–429.

Kohn, M. J., & Cerling, T.E. (2002). Stable Isotope Compositions of Biological Apatite. *Mineral. Geochemistry, 48*, 455–488.

Kohn, M. J., Schoeninger, M. J., & Valley, J. W. (1996). Herbivore tooth oxygen isotope compositions: effects of diet and physiology. *Geochimica et Cosmochimica Acta, 60* (20), 3889–3896.

Kolodny, Y., Luz, B., & Navon, O. (1983). Oxygen isotope variations in phos- phate ofbiogenic apatites, I. Fish bone apatite—rechecking the rules of the game. *Earth Planet Sci Lett., 64*, 398–404.

Langer, M. C., Bittencourt, J. S., & Schultz, C. L. (2010). A reassessment of the basal dinosaur Guaibasaurus candelariensis, from the Late Triassic Caturrita Formation of south Brazil. *Earth and Environmental Science Transactions of the Royal Society of Edinburgh, 101*, 301–332.

Lécuyer, C. (2004). Oxygen Isotope Analysis of Phosphate, in: Handbook of Stable Isotope Analytical Techniques. Elsevier, Amsterdam, 482–496.

Lécuyer, C., Grandjean, P., & Sheppard, S. M. F. (1999). Oxygen isotope exchange between dissolved phosphate and water at temperatures ⩽ 135°C: inorganic versus biological fractionations. *Geochim Cosmochim Acta, 63*, 855-862.

Lécuyer, C., Bogey, C., Garcia, J.P., Grandjean, P., Barrat, J.A., Floquet, M., …, Pereda-Superbiola, X. (2003). Stable isotope composition and rare earth element con- tent ofvertebrate remains from the Late Cretaceous ofnorthern Spain (Laño): did the environmental record survive? *Palaeogeography, Palaeoclimatology, Palaeoecology, 193*, 457–471.

Lécuyer, C., Grandjean, P., O'Neil, J.R., Capetta, H., & Martineau, F. (1993). Thermal excursions in the ocean at the Cretaceous–Tertiary boundary (northern Morocco): the $\delta^{18}O$ record of phosphatic fish debris. *Palaeogeogr. Palaeoclimatol. Palaeoecol, 105*, 235-243.

Leong G. C. (1995). Certificate Physical and Human Geography. *Oxford; 1st edition (October 1, 1995)*.

Longinelli, A. (1984). Oxygen isotopes in mammal bone phosphate: a new tool for paleohydrological and paleoclimatological research? *Geochim Cosmochim Acta, 48*, 385–390.

Luo, Z. X., & Wu, X. C. (1994). The small tetrapods of the Lower Lufeng Formation, Yunnan, China; pp. 251-270 in N. C. Fraser and H-D. Sues (eds.), In the Shadow of the Dinosaurs: Early Mesozoic Tetrapods. Cambridge University Press, Cambridge.

Luz, B., Kolodny, Y., & Horowitz, M. (1984) Fractionation ofoxygen isotopes between mammalian bone-phosphate and environmental drinking water. *Geochim Cosmochim Acta, 48*,1689–1693.

Morettini, E., Santantonio, M., Bartolini, A., Cecca, F., Baumgartner, P.O., & Hunziger, J.C. (2002). Carbon isotope stratigraphy and carbonate production during the Early Jurassic: examples from the Umbria-Marche-Sabina Appenines (central Italy). *Palaeogeogr. Palaeoclimatol. Palaeoecol., 184*, 251–273.

Murphy, B. P., Andersen, A. N., & Parr, C. L. (2016). The underestimated biodiversity of tropical grassy biomes. *Philosophical Transactions of the Royal Society B: Biological Sciences*, 371(1703).

Passey, B. H., Robinson, T.F., Ayliffe, L. K., Cerling, T. E., Sponheimer, M., Dearing, M. D., …,

Ehleringer, J.R. (2005). Carbon isotope fractionation between diet, breath CO_2, and bioapatite in different mammals. *Journal of Archaeological Science, 32*(10): 1459–1470.

Passey, B. H., Cerling, T. E., Perkins, M. E., Voorhies, M. R., Harris, J. M., & Tucker, S. T. (2002). Environmental Change in the Great Plains: An Isotopic Record from Fossil Horses. *The Journal of Geology, 110*(4), 123–140.

Patterson, B., & Olson, E. C. (1961). A triconodont mammal from the Triassic of Yunnan. In Vandebroek G, ed. International Colloquium on the Evolution of Lower and Non-specialized Mammals.

Porada, P., Lenton, T. M., Pohl, A., Weber, B., Mander, L., Donnadieu, Y., ... & Kleidon, A. (2016). High potential for weathering and climate effects of non-vascular vegetation in the Late Ordovician. *Nature Communications*, *7*(1), 1-13.

Rahmaniati, M., Eryando, T., Susanna, D., Pratiwi, D., Nugraha, F., & Riandi, U. (2014). The utilization of Standard Deviational Ellipse (SDE) model for the analysis of dengue fever cases in Banjar city 2013. *Aspirator, 6*, 21–28.

Rey, K. vin, Amiot, R., & Fourel, F. (2017). Oxygen isotopes suggest elevated thermometabolism within multiple Permo-Triassic therapsid clades Oxygen isotopes suggest elevated thermometabolism within multiple Permo- Triassic therapsid clades. eLife Sci.

Rigney, H. W. (1963). A specimen of Morganucodon from Yunnan. *Nature, 197*, 1122-1123.

Sekiya, T. (2010). A new prosauropod dinosaur from Lower Jurassic in Lufeng of Yunnan. *Global Geology, 29*, 6–15.

Simmons, D. J. (1965). The non-therapsid reptiles of the Lufeng Basin, Yunnan, China. *Fieldiana: Geology, 15*, 1-93.

Spoetl, C., & Vennemann, T.W. (2003). Continuous-flow isotope ratio mass spectrometric analysis of carbonate minerals. *Rapid Commun. Mass Spectrom., 17*, 1004–1006.

Stanton-Thomas, K.J., & Carlson, S.J. (2004). Microscale $\delta^{18}O$ and $\delta^{13}C$ isotopic analysis of an ontogenetic series of the hadrosaurid dinosaur Edmontosaurus: Implications for physiology and ecology. *Palaeogeogr Palaeoclimatol Palaeoecol., 206*, 257–287.

Straight, W. H., Barrick, R. E., & Eberth, D. A. (2004). Reflections of surface water, seasonality and climate in stable oxygen isotopes from tyrannosaurid tooth enamel. *Palaeogeography, Palaeoclimatology, Palaeoecology., 206*(3-4), 239-256.

Sun, A. L., & K. H. Cui. (1986). A brief introduction to the Lower Lufeng saurischian fauna (Lower Jurassic: Lufeng, Yunnan. People's Republic of China), 275-278 in K. Padian (ed.), The Beginning of the Age of Dinosaurs: Faunal Change Across the Triassic-Jurassic Boundary. Cambridge University Press, Cambridge.

Torsvik, T. H. & Cocks, L. R. M. (2016). *Earth history and palaeogeography*. Cambridge University Press.

Tütken, T., Pfretzschner, H. U., Vennemann, T. W., Sun, G., & Wang, Y. D. (2004). Paleobiology and skeletochronology of Jurassic dinosaurs: Implications from the histology and oxygen isotope compositions of bones. *Palaeogeogr. Palaeoclimatol. Palaeoecol., 206*, 217–238.

Tütken, T. (2011). The diet of sauropod dinosaurs: implications from carbon isotope analysis of teeth, bones, and plants, in: Klein, N., Remes, K., Sander, M. (Eds.), Biology of the Sauropod Dinosaurs: Understanding the Life of Giants. Indiana University Press, Bloomington, 57–79.

Utescher, T., Ashraf, A. R., Kern, A. K., & Mosbrugger, V. (2020). Diversity patterns in microfloras recovered from Miocene brown coals of the lower Rhine Basin reveal distinct coupling of the structure of the peat - forming vegetation and continental climate variability. *Geological Journal*.

Vennemann, T. W., Hegner, E., Cliff, G., & Benz, G. W. (2001). Isotopic composition of recent shark teeth as a proxy for environmental conditions. *Geochimica Et Cosmochimica Acta, 65*,1583–1599.

Grafenstein, U. V., Erlenkeuser, H., Mueller, J., Trimborn, P., & Alefs, J. (1996). A 200 year mid-European air temperature record preserved in lake sediments; an extension of the δ18OP–air temperature relation into the past. *Geochim. Cosmochim. Acta, 60*, 4025–4036.

Wang, Y. M., You, H. L., & Wang, T. (2017). A new basal sauropodiform dinosaur from the Lower Jurassic of Yunnan Province, China. *Sci. Rep., 7*, 41881.

William, W. H., & Sascha, F. (2012). New thoughts about the Cretaceous climate and oceans. *Earth-Science Reviews, 115*, 262-272.

Wu, X., Currie, P.J., Dong, Z., Pan, S., & Wang, T. (2009). A new theropod dinosaur from the Middle Jurassic of Lufeng, Yunnan, China. *Acta Geologica Sinica, 83*, 9–24 (In Chinese).

Wu, X. C. (1991). The comparative anatomy and systematics of Mesozoic sphenodontidans. Ph.D. dissertation, McGill University, Montreal, 229.

Wu, X. C., & Chatterjee, S. (1993). Dibothrosuchus elaphros, a crocodylomorph from the Lower Jurassic of China and the phylogeny of the Sphenosuchia. *Journal of Vertebrate Paleontology, 13* (1), 58-89.

Noto, C. R., & Grossman, A. (2010). Broad scale patterns of Late Jurassic dinosaur paleoecology. PLoSONE5: e12553.

Xing, L.D., Bell, P.R., Rothschild, B.M., Ran, H., Zhang, J.P., Dong, Z.M., ..., Currie, P.J. (2013). Tooth loss and alveolar remodeling in Sinosaurus triassicus (Dinosauria: Theropoda) from the lower jurassic strata of the Lufeng Basin, China. *Chinese Sci. Bull., 58*, 1931–1935.

Young, C. C. (1941a). A complete osteology of Lufengosaurus huenei Young (gen. et sp. nov.) from Lufeng, Yunnan, China. *Palaeontologica Sinica (Series C), 7*, 1–53.

Young, C. C. (1941b). Gyposaurus sinensis (sp. nov.), a new Prosauropoda from the Upper Triassic beds at Lufeng, Yunnan. *Bulletin of Geology Society of China, 21*, 205-253.

Young, C. C. (1942). Yunnanosaurus huangi (gen. et sp. nov.), a new Prosauropoda from the Red Beds at Lufeng, Yunnan. *Bulletin of the Geological Society of China, 22*, 63-104.

Young, C. C. (1947). On Lufengosaurus magnus Young (sp. nov.) and additional finds of Lufengosaurus huenei Young. *Palaeontologica Sinica (Series C), 12*, 1-53.

Young, C.C. (1951). The Lufeng saurischian fauna. *Palaeontologica Sinica (Series C), 13*, 1–96.

Zazzo, A., Lécuyer, C., & Mariotti, A. (2004a). Experimentally-controlled carbon and oxygen isotope exchange between bioapatites and water under inorganic and microbially-mediated conditions. *Geochim Cosmochim Acta, 68*, 1–12.

Zazzo, A., Lécuyer, C., Sheppard, S. M. F., Grandjean, P., & Mariotti, A. (2004b). Diagenesis and the reconstruction of paleoenvironments: a method to restore original $d^{18}O$ values of carbonate and phosphate from fossil tooth enamel. *Geochimica Et Cosmochimica Acta., 68*, 2245–2258.

Zhang, F., & Cui, G. (1983). New material and new understanding of Sinoconodon. *Vertebrata Palasiatica, 21*, 32-41.

Zhang, L., Wang, C., Li, X., Cao, K., Song, Y., Hu, B., …, Cao, S. (2016). A new paleoclimate classification for deep time. *Palaeogeogr. Palaeoclimatol. Palaeoecol., 443*, 98–106.

677 Zhang, Y. H., & Yang, Z. L. (1995). A new complete osteology of Prosauropoda in Lufeng Basin,
678 Yunnan, China: Jingshanosaurus. (Yunnan Publishing House of Science and Technology).

Figure Captions

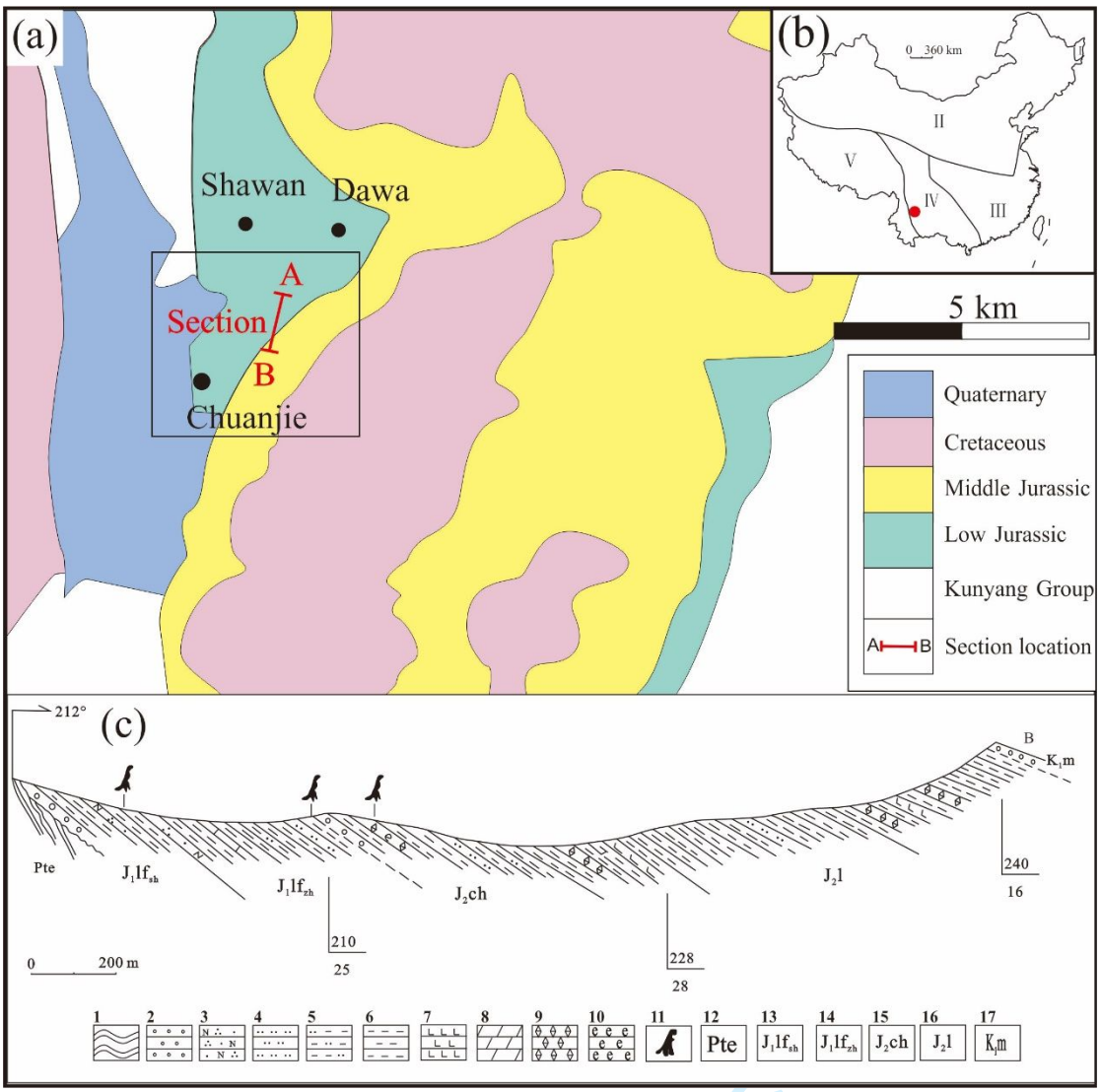

Figure 1 Schematic geological map of the Lufeng Basin. (a) The geological setting of the Lufeng Basin. (c) The study section from A to B. 1 Killas; 2 Basal conglomerates; 3 Arkosic sandstone; 4 Siltstone; 5 Argillaceous siltstones; 6 Mudstone; 7 Calcareous mudstones; 8 Marlstone; 9 Micritic limestones; 10 Bioclastic limestone; 11 Dinosaur fossils; 12 Kunyang group; 13 Shawan member in Low Jurassic; 14 Zhangjiaao member in Low Jurassic; 15 Chuanjie member in Middle Jurassic; 16 Laoluocun member in Middle Jurassic; 17 Matoushan Formation in Cretaceous. Modified after Wang et al. (2017) and Fang et al. (2000). (b) The Jurassic climatic zones in China, modified after Deng et al. (2007). (I) Wushuli warm-cool climatic region in Eastern Heilongjiang, (Ⅱ) North China warm-temperate humid climatic region, (Ⅲ) Southeast China tropic-subtropical humid climatic region, (IV)

689 Southwest China tropic-subtropical semi-arid and semi-humid climatic region, (Ⅴ) Tibetwestern Yunnan tropical

690 oceanic arid climatic region.

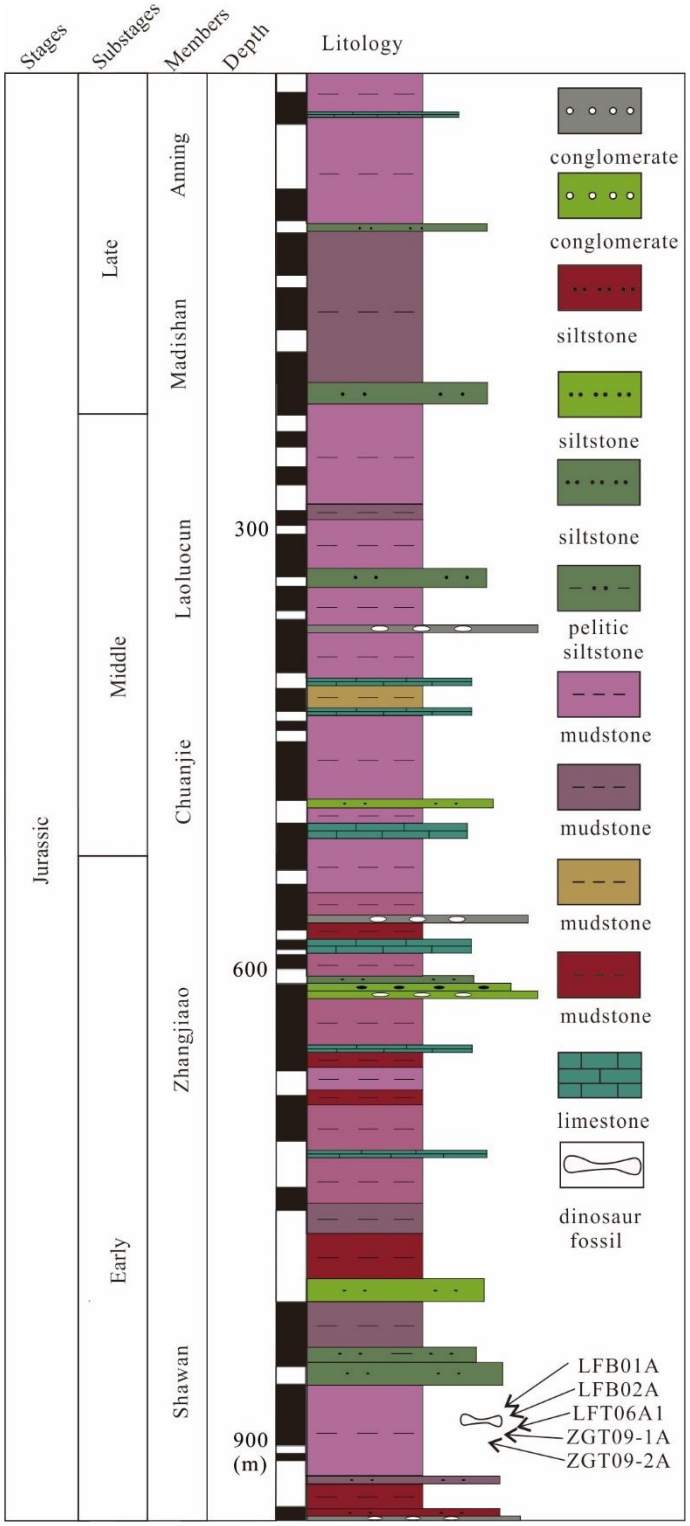

691

692 **Figure 2 Lithological column of the Lufeng Basin**. The samples were recovered from the lower part of the

693 Shawan Member.

694

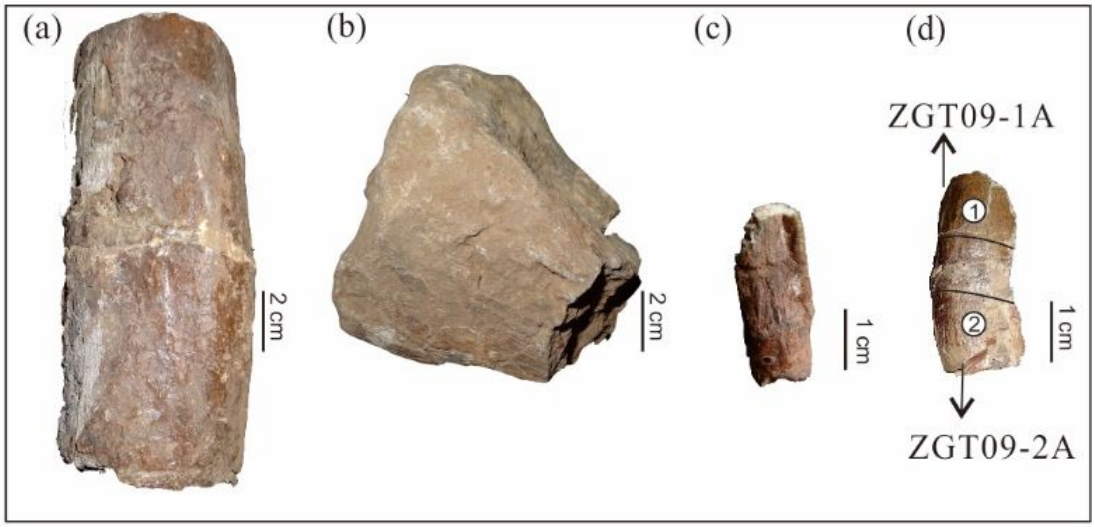

695

696 **Figure 3 Teeth and bones analysed in this study.** (a-b) The basal sauropodiform dinosaur bones; (c) The basal

697 sauropodiform dinosaur tooth; (d) The *S.triassicus* tooth.

Table 1 The oxygen isotope compositions of dinosaurs' phosphate and carbonate.

Sample ID	Material	Taxa	Ecology[a]	$\delta^{18}O_p$ (‰, VSMOW)		$\delta^{13}C_{CO3}$ (‰, VPDB)		$\delta^{18}O_{CO3}$ (‰, VSMOW)		$CaCO_3$ (Wt%)
				$\delta^{18}O_{cor}$	SD	$\delta^{13}C_{CO3}$	SD	$\delta^{18}O_{CO3}$	SD	
LFB01A	bone	basal sauropodiform	herb.	15.9	0.1	-10.6	0.1	19.9	0.1	3.1
LFB02A	bone	basal sauropodiform	herb.	16.4	0.1	-9.2	0.1	21.5	0.1	2.1
LFT06A1	teeth crown	basal sauropodiform	herb.	20.5	0.2	-8.7	0.1	23.7	0.1	2.6
ZGT09-1A	teeth apex	Sinosaurus	carn.	20.4	0.2	-7.8	0.1	27.2	0.1	12.1
ZGT09-2A	teeth cervix	Sinosaurus	carn.	17.0	0.1	-7.1	0.1	21.0	0.1	2.6

[a] *herb*. Herbivorous, *carn*. Carnivorous.

Table 2 The mean values of $\delta^{18}O_w$ and MAT in Lufeng Locality

Taxa	$\delta^{18}O_{PO4}$ (‰, VSMOW)		$\delta^{18}O_{PO4}$ (‰, VSMOW)		Estimated $\delta^{18}O_w$ (‰, VSMOW)		MAT (℃)	
	Mean	SD	Mean	SD	Mean	SD	Mean	SD
basal sauropodiform dinosaur	17.6	0.2	18.2	0.3	-3.9	±0.7	21	±0.8
S.triassicus	18.7	0.2						

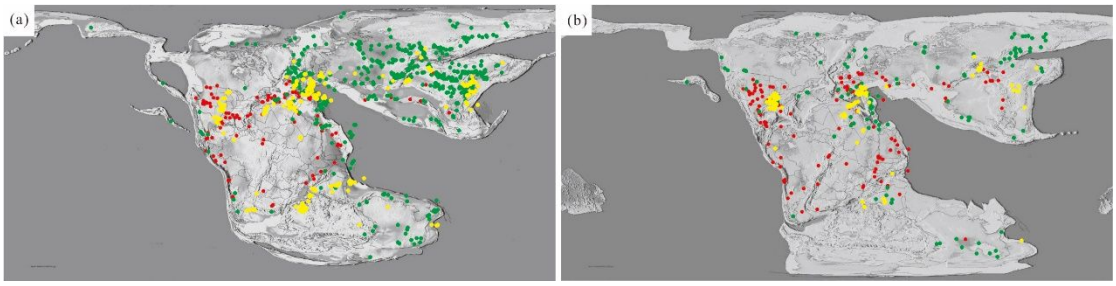

Figure 4. The distributions of dinosaur fossils and climatically sensitive sediments during the (a) Early - middle Jurassic and (b) Late Jurassic. The yellow dots represent the dinosaur fossil sites. The red and green dots represent the arid and humid climatically sensitive deposits, respectively.

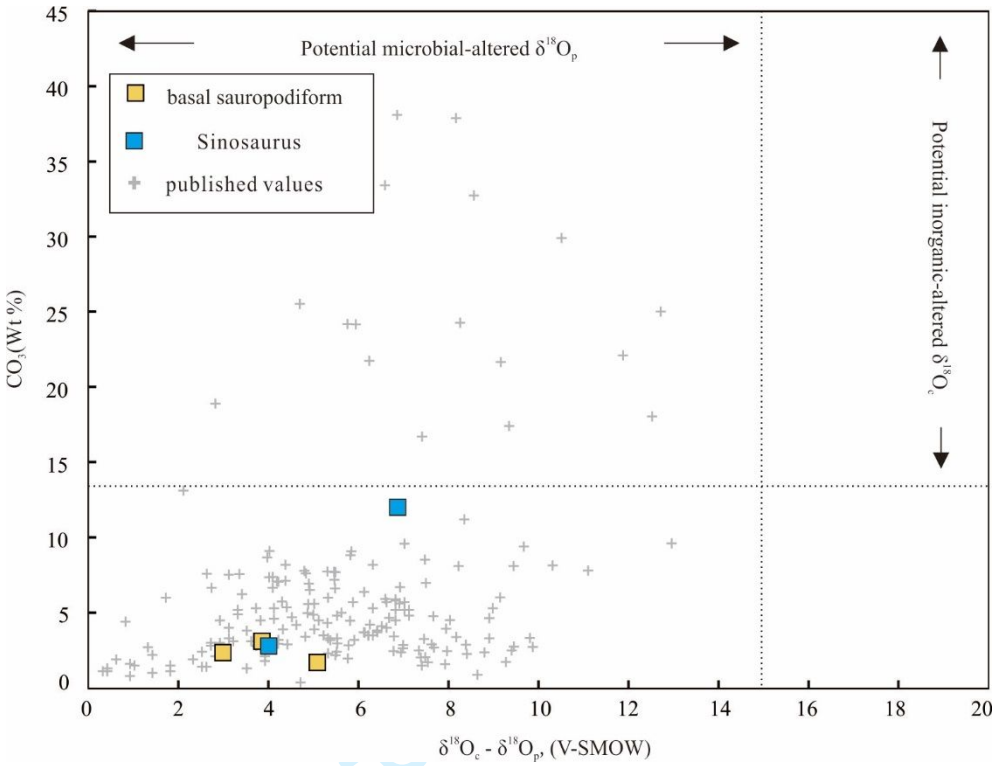

706

707 **Figure 5 The assessment of the preservation condition.** The $\delta^{18}O_c$-$\delta^{18}O_p$ differences between teeth and bones

708 plotted against the structural carbonate content (wt %) of apatite. Modified after Amiot et al. (2015) and Rey et al.

709 (2017).

710

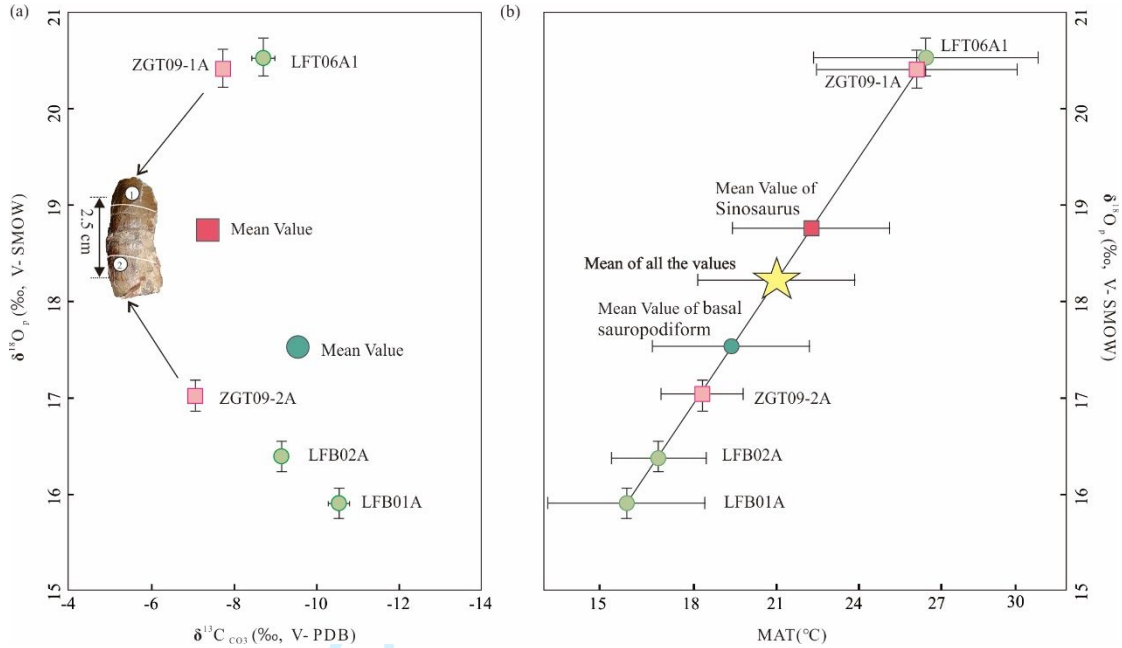

Figure 6 The stable isotope compositions of the dinosaur fossils. (a) The mean $\delta^{18}O_p$ (‰, VSMOW) vs $\delta^{13}C_{CO3}$ (‰, VPDB) values. (b) The temperature vs $\delta^{18}O_p$ (‰, VSMOW). The red squares represent Sinosaurus tooth, the green circles represent the basal sauropodomorphs, and the yellow star represents the mean MAT.

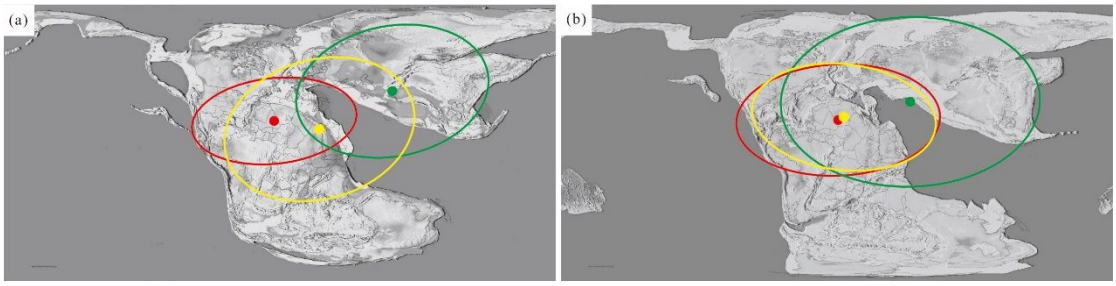

Figure 7 The standard elliptic and center of gravity of dinosaur and climatic proxies. (a) Early-middle Jurassic and (b) Late Jurassic. The yellow elliptic represents dinosaur data. The red elliptic represents the arid climatic data and the green represents humid climatic data. The corresponding colored circles represent the position of the center of elliptic gravity.

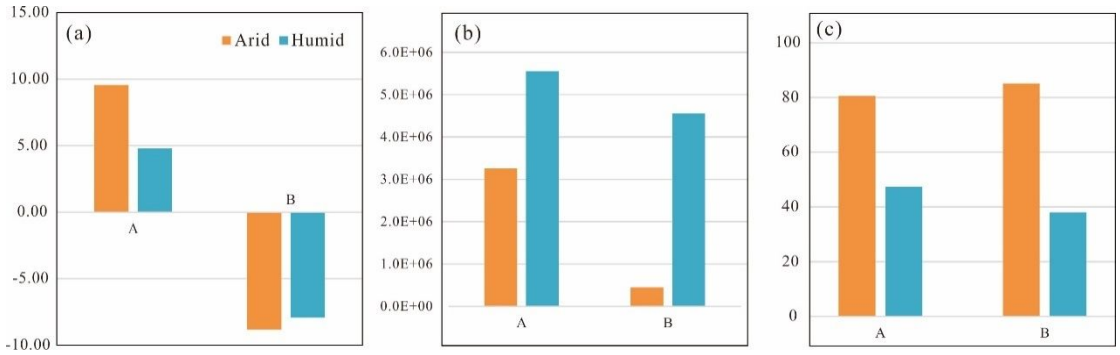

Figure 8 Summarizes the bar chart of SDE spatial analysis in Jurassic. (a) Bar chart of SDE rotation of D(A-D) and D(H-D). (b) Bar chart of the distance between the SDE gravity of A-D and H-D. (c) Bar chart of percentage between the intersection area of A-D and H-D.